

Probing Rotational Dynamo Extremes: X-ray and Optical Spectroscopy of the 0.5 Day Period Eclipsing Binary, HD 79826

David P. Huenemoerder¹, Joy S. Nichols², David DePalma²,
David Garcia-Alvarez³, Norbert S. Schulz¹

¹*MIT Kavli Institute for Astrophysics and Space Research*

²*Harvard-Smithsonian Center for Astrophysics*

³*Instituto de Astofísica de Canarias*

Abstract. The highly modulated optical light curve of HD 79826 (spectral types G5+M5) was discovered in the *Chandra* guide-star light curves, indicating a period of about 0.5 days, a strong and migrating distortion wave, and a shallow eclipse. We subsequently obtained simultaneous *Chandra* high resolution X-ray spectra and optical photometry, along with contemporaneous ground-based photometry and spectra. X-ray rotational or eclipse modulation was totally obscured by X-ray variability and flares. X-ray spectra are characterized by coronal emission near the saturation limit of $L_x/L_{\text{bol}} = 10^{-3}$. Optical spectra show extremely rotationally broadened features, variable with orbital phase. Optical light curves show the modulation to be not only rapidly migrating in phase, but also of variable amplitude. We characterize the X-ray emission through measurements of line widths, velocities, and fluxes, and provide coronal plasma models. This star is near or at the limits of dynamo saturation, and since it is partially eclipsing, has potential to be well characterized in terms of fundamental stellar parameters.

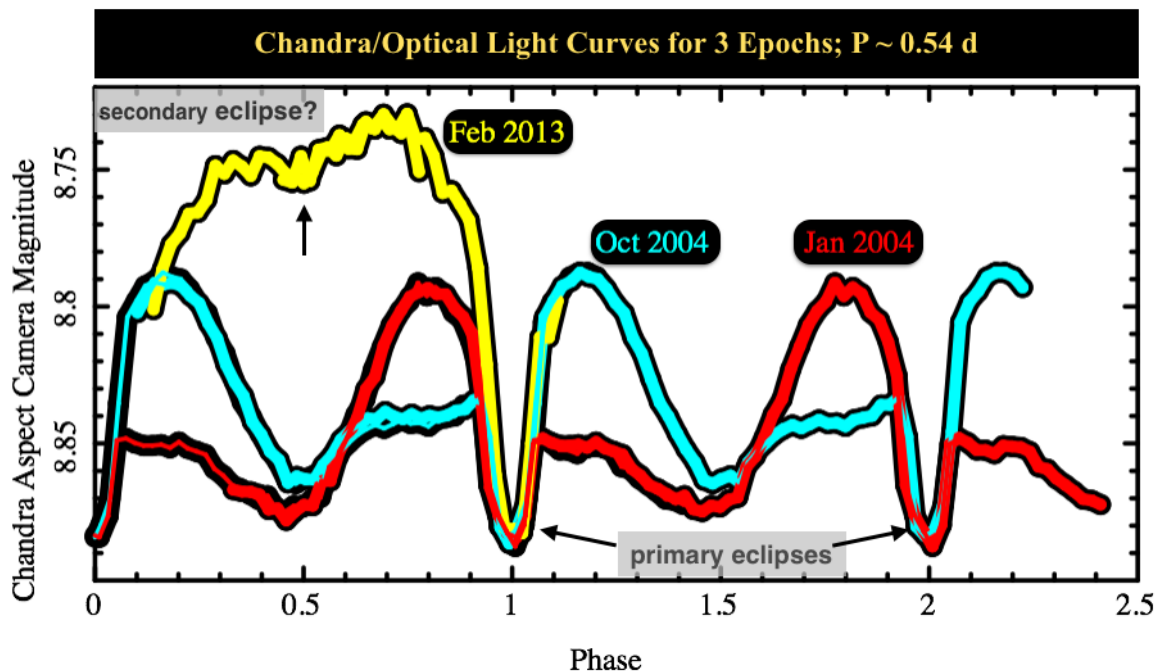


Figure .1: *Chandra* aspect camera optical light curves of HD 79826. The cyan and red curves each cover more than two cycles (data have *not* been replicated for phases greater than 1.0).

1. *Chandra* Optical Light Curves

HD 79826 was discovered to be a short period eclipsing variable with a rapidly migrating distortion (“spot”) wave in the *Chandra* Variable Guide Star Catalog¹ of Nichols et al. (2010). In 2004 it was observed twice for over two cycles each time. In 2013, it was observed both as a guide star and as the primary X-ray target of the *Chandra* High Energy Grating Spectrometer (HETG). Figure .1 shows three *Chandra* optical light curves indicating the primary eclipse and the rapidly changing distortion wave.

An estimate of the system geometry and basic parameters are shown in Figure .2, based on the observed period and nominal spectral types.

2. *Chandra*/HETG X-ray Light Curves

The X-ray light curves were derived from the February 2013 *Chandra*/HETG observations of HD 79826 (observation identifiers 15272 and 15612) in which the star was also used as an aspect camera guide star. Light curves were extracted from the HETG first order events in soft, hard, and full bands² The *Chandra*/HETG X-ray light curves show strong variability.

¹<http://cxc.harvard.edu/vguide>

²Curves were extracted using the “aglc” package; <http://space.mit.edu/cxc/analysis/aglc/>.

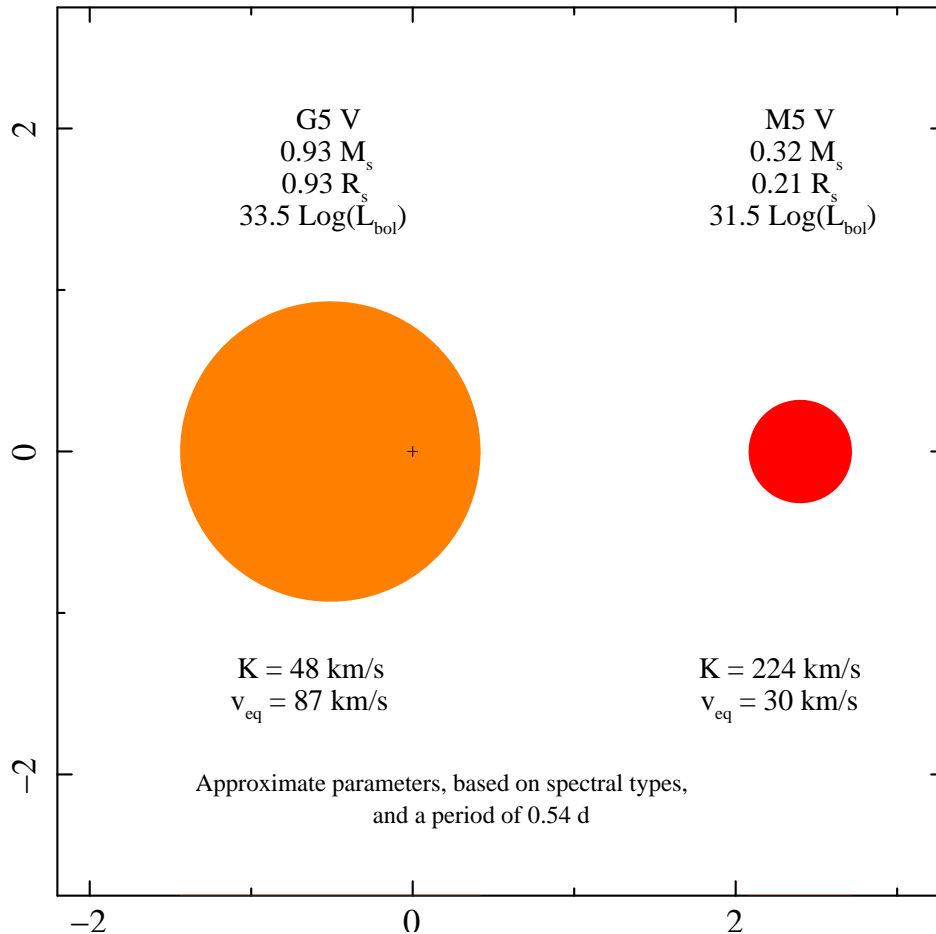


Figure .2: Approximate binary system geometry and parameters, based on nominal spectral types and the observed period. Axes' units are in solar radii.

However, this is primarily due to a strong flare, seen not only in the sharp jump in count rate, but also in a hardness ratio. Figure .3 shows the HETG light curves. The flare, unfortunately, occurred right through primary eclipse, hiding any modulation of coronal emission by the secondary. Figure .4 shows the phased simultaneous X-ray and optical light curves.

3. X-ray Spectra

The *Chandra*/HETG X-ray spectrum is typical of coronal emission with a host of H- and He-like emission lines of abundant elements, as well as Fe-L lines. Figure .5 shows mean flux for the two observations. A 3-temperature component APEC (Smith et al. 2001; Foster et al. 2012) model follows the data very well. The lines show no width or shift in excess of instrumental resolution, indicating that the primary (G5 V) star dominates the X-ray emission. ($\Delta v = 25 \pm 35 \text{ km s}^{-1}$; $FWHM < 280 \text{ km s}^{-1}$).

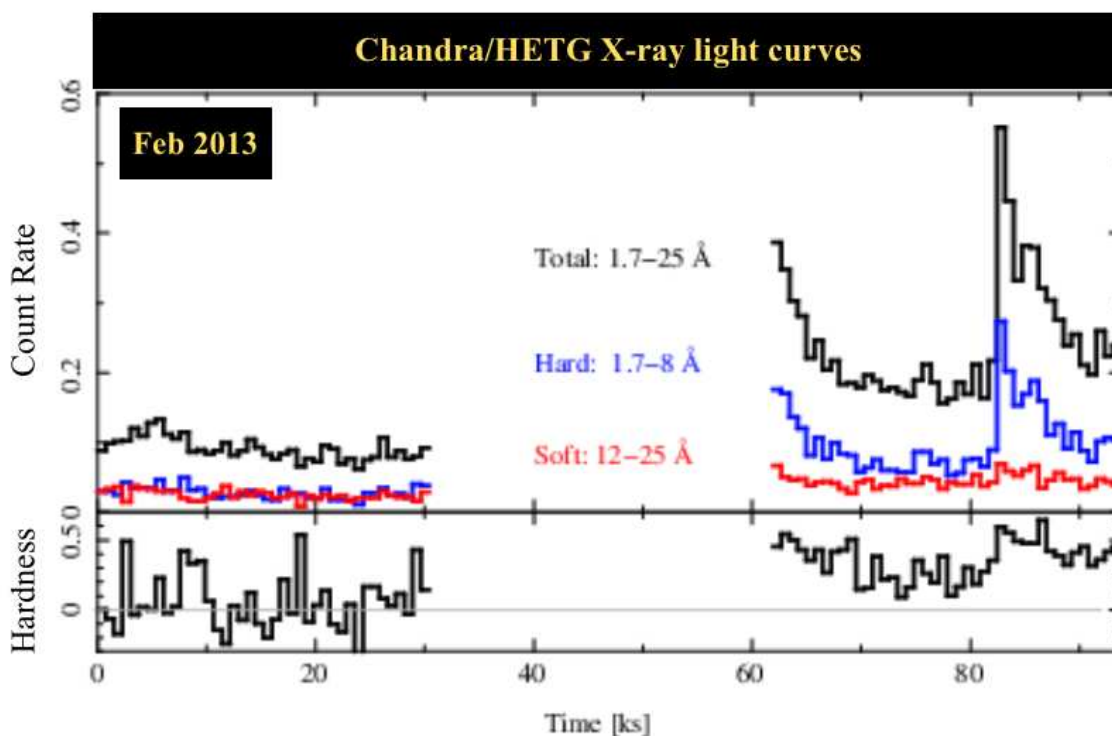


Figure .3: X-ray light curves from HETG events. The time is from the start of the first observation, and the count rate is for the sum of the HEG and MEG first orders. Black (top curve) is the full HETG band, blue (middle curve) a hard band, and red (lower) a soft band. The lower panel shows a hardness ratio, defined as $(hard - soft)/(hard + soft)$.

The higher flux HETG spectrum is characteristic of stellar and solar flares in the sharp rise in count rate with slower decay, as well as in spectral changes indicative of high temperature plasmas, namely an enhanced short-wavelength continuum ($2 - 10 \text{ \AA}$) and strong lines of highly ionized iron. Figure .6 shows the flare and low-state spectra. Discrete 3-temperature plasma model fits to the flare and low-state spectra yield the temperature and emission measure which show (Figure .6, right panel) the large enhancement in high temperature plasma typical of flares.

4. Optical Spectra

We have obtained high resolution optical spectra, monitored contemporaneously with the X-ray spectra. Figure .7 shows two examples from the series, showing the $H\alpha$ and $H\beta$ regions. Lines are highly broadened, as expected for rapidly rotating stars. We will model these spectra by fitting templates and will derive radial and rotational velocities and relative intensity weights, and thereby improve the binary systems basic parameters.

5. Relevance

Compared to other coronally active stars, HD 79826 is among the most active, being near or at the saturation limit, and showing no sign of “supersaturation” at the shortest periods. Being a detached (probably) and eclipsing binary, it can provide an important benchmark at the extreme limit of stellar magnetic dynamos. Figure .8 shows the location of the HD 79826 among other stars.

Acknowledgements: This work was supported by NASA through the Smithsonian Astrophysical Observatory (SAO) contract SV3-73016 for the Chandra X-Ray Center and Science Instruments.

References

- Foster, A. R., Ji, L., Smith, R. K., & Brickhouse, N. S. 2012, ApJ, 756, 128
- Nichols, J. S., Henden, A. A., Huenemoerder, D. P., Lauer, J. L., Martin, E., Morgan, D. L., & Sundheim, B. A. 2010, ApJS, 188, 473
- Smith, R. K., Brickhouse, N. S., Liedahl, D. A., & Raymond, J. C. 2001, ApJ, 556, L91
- Szczygiel, D. M., Socrates, A., Paczyński, B., Pojmański, G., & Pilecki, B. 2008, AcA, 58, 405

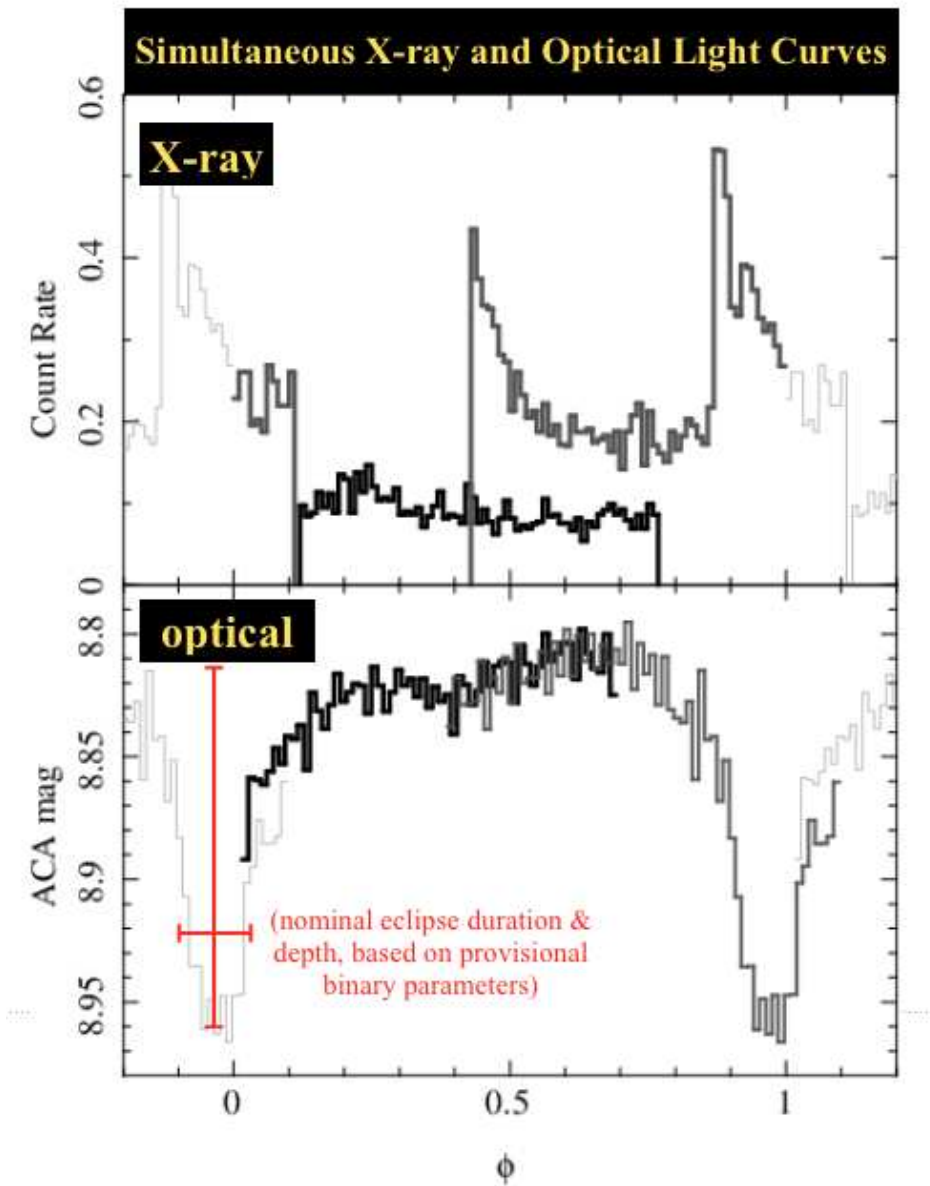


Figure 4: Phased simultaneous X-ray and optical light curves from *Chandra* HETG and aspect camera. Black and dark gray show the data from the two observations, while light gray is used to show duplicated data over wrapped phases. The red cross denotes the nominal eclipse depth and width expected based solely on the spectral types and observed period, and not an eclipsing binary light curve solution.

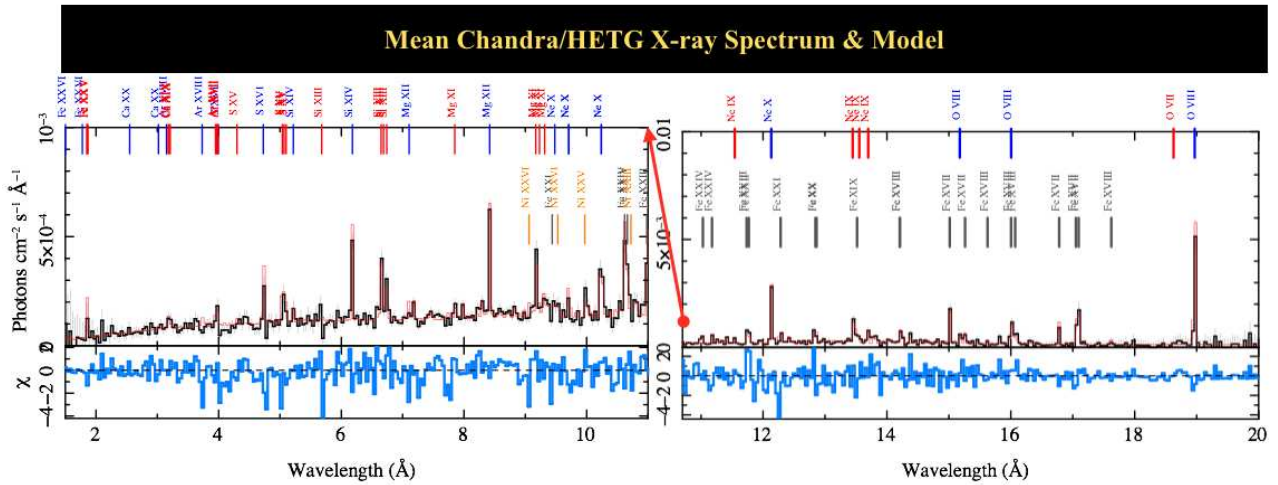


Figure .5: The HETG spectrum of HD 79826 (black histogram), an APEC model (red histogram) and residuals (blue, lower panel). H-like lines are labeled in blue, He-like in red. Other Fe lines are labeled in gray. The range of the y -axis range in right panel is 10 times that of the left.

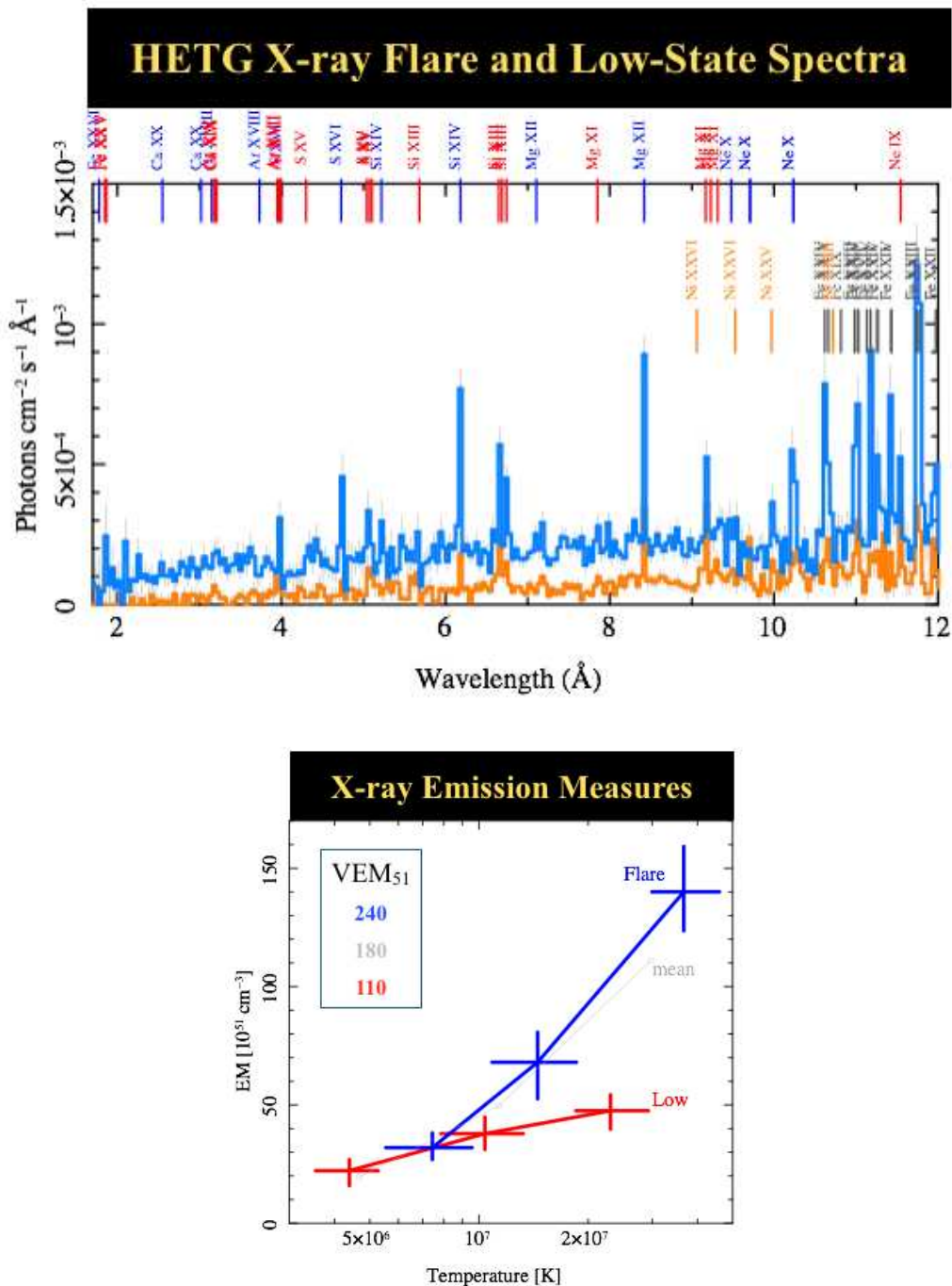


Figure .6: On the top is the HETG spectrum during the flares (blue; observation shown in dark gray in Figure .4) and the low-state spectrum (orange; black in Figure .4). The bottom panel shows the temperatures and emission measures of 3-temperature APEC model fits to the flare (blue) and low (red) states. The inset table in the bottom panel gives integrated emission measures for each state (other values for comparison: Capella (moderate activity): 50, and II Peg (high activity): 800).

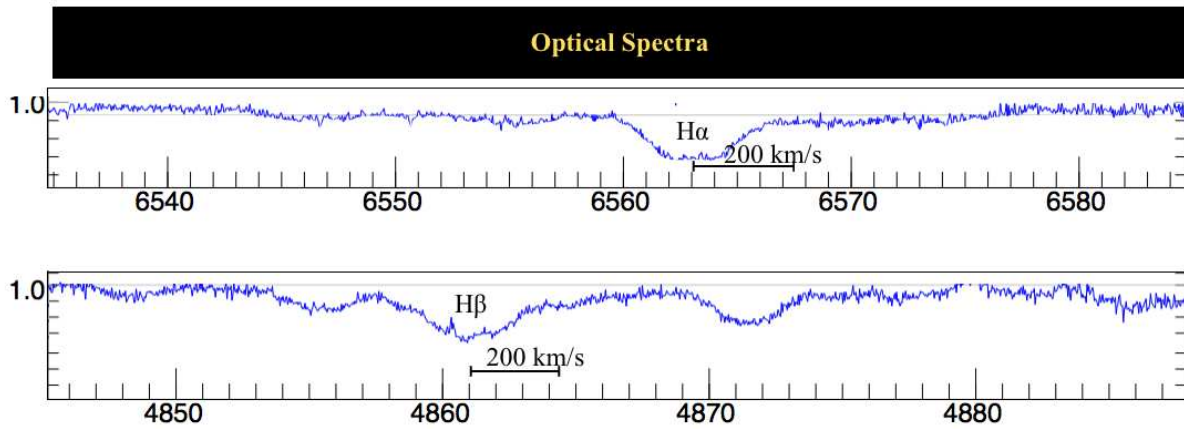


Figure .7: Example H α (top) and H β spectra obtained contemporaneously with the X-ray spectra. Lines are very broad. A bar of length 200 km s⁻¹ is shown for reference, which is the approximate maximum velocity separation of the two components, though it may be difficult to detect the fainter M5 star’s signature.

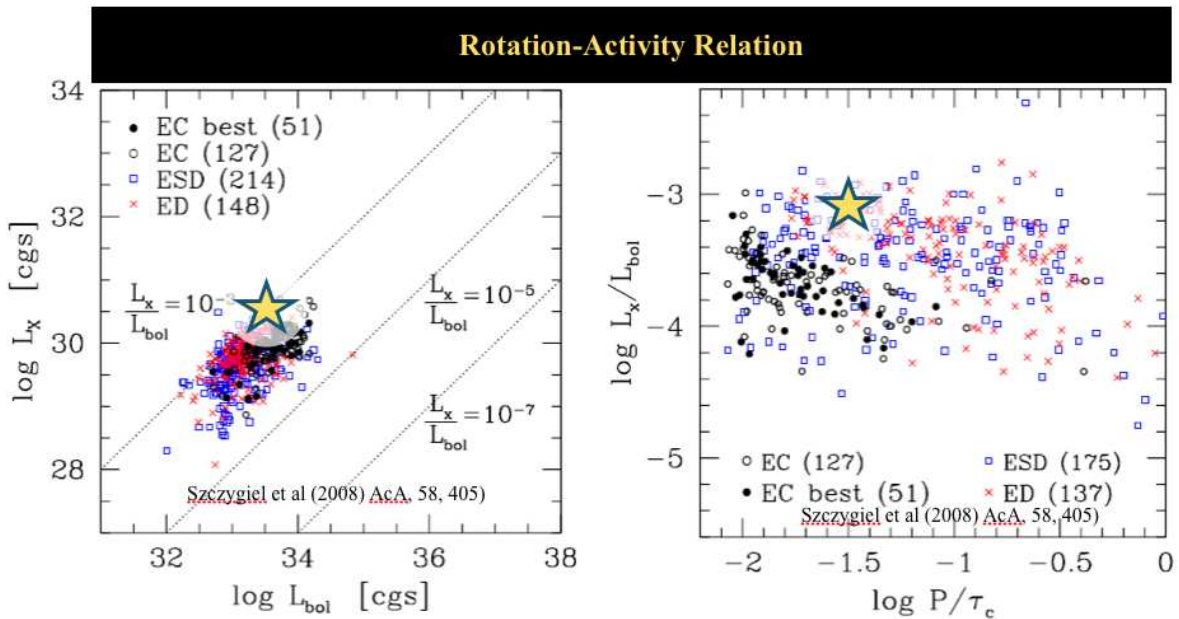


Figure .8: The location of HD 79826 is shown (big yellow star) on the distribution of other active stars, from [Szczyciel et al. \(2008\)](#). In the right-hand panel, the x -axis is the Rossby number, the ratio of the rotational period, P , to convective turnover time, τ_c .

